Circulating extracellular vesicles as non-invasive biomarker of rejection in heart transplant

Circulating Extracellular Vesicles as a Noninvasive Biomarker of Rejection in Heart Transplant

C. Castellani[1*], J. Burrello[2*], M. Fedrigo[1], A. Burrello,[3] S. Bolis[2],

D. Di Silvestre[4], F. Tona[5], T. Bottio[5], V.Biemmi[2,7], G. Toscano[5], G. Gerosa[5], G. Thiene[1],

C. Basso[1], S.L. Longnus[6], G. Vassalli[2,7], A. Angelini[1#], L. Barile[2,7,8#].

(1) Cardiovascular Pathology and Pathological Anatomy, Department of Cardiac, Thoracic, Vascular Sciences and Public Health, University of Padova, Padova, Italy. (2) Laboratory of Cellular and Molecular Cardiology and Laboratory for Cardiovascular Theranostics, Cardiocentro Ticino Foundation, Lugano, Switzerland. (3) Department of Electrical, Electronic and Information Engineering "Guglielmo Marconi" (DEI), University of Bologna, Italy. (4) Proteomics and Metabolomic Lab, ITB-CNR, Segrate, Italy. (5) Division of Cardiac Surgery, Dept. of Cardiac-Thoracic Vascular Sciences and Public Health, University of Padua, Italy. (6) Department of Cardiovascular Surgery, Inselspital, Bern University Hospital, Bern, Switzerland. (7) Faculty of Biomedical Sciences, Università Svizzera Italiana, Lugano, Switzerland. (8) Institute of Life Science, Scuola Superiore Sant'Anna, Pisa, Italy.

[*]Equally contributing first authors. #Equally contributing last authors.

Manuscript word count: 6990 including references and figure captions. Abstract word count: 250

Number of Tables: 1; Number of Figures: 6.

Supplementary data: 11 Supplementary Tables and 2 Supplementary Figures.

Addresses for correspondence:

Annalisa Angelini (email: annalisa.angelini@unipd.it) – Department of Cardiac, Thoracic, Vascular Sciences and Public Health, University of Padova - Via A. Gabelli 61, 35121 – Padova (Italy)

Lucio Barile (email: lucio.barile@cardiocentro.org) – Laboratory for Cardiovascular Theranostics, Cardiocentro Ticino Foundation - Via Tesserete 48, 6900 – Lugano (Switzerland).

ABSTRACT

Aims – Circulating extracellular vesicles (EV) are raising considerable interest as a non-invasive diagnostic tool as they are easily detectable in biological fluids and contain specific set of nucleic acids, proteins, and lipids reflecting pathophysiological conditions. We aimed to investigate differences in plasma-derived EV surface-protein profile as biomarker to be used in combination with endomyocardial biopsies (EMB) for the diagnosis of allograft rejection.

Methods and results – Plasma was collected from 90 patients (53 training cohort, 37 validation cohort) prior to EMB. EV concentration was assessed by nanoparticle tracking analysis. EV surface antigens were measured using a multiplex flow cytometry assay comprising 37 fluorescently labelled capture bead populations coated with specific antibodies directed against respective EV surface epitopes. The concentration of EV was significantly increased and their diameter decreased in patients undergoing rejection as compared to negative ones. The trend was highly significant for both antibody-mediated rejection (AMR), and acute cellular rejection (P<0.001). Among EV-surface markers, CD3, CD2, ROR1, SSEA-4, HLA-I, and CD41b were identified as discriminants between controls and ACR, whereas HLA-II, CD326, CD19, CD25, CD20, ROR1, SSEA-4, HLA-I, and CD41b discriminated controls from patients with AMR. ROC curves confirmed a reliable diagnostic performance for each single marker (AUC range 0.727-0.939). According to differential EV-marker expression, a diagnostic model was built and validated in an external cohort of patients. Our model was able to distinguish patients undergoing rejection from those without rejection. The accuracy at validation in an independent external cohort reached 86.5%. Its application for patient management has the potential to reduce the number of EMBs. Further studies in a higher number of patients are required to validate this approach for clinical purpose.

Conclusions - Circulating EV are highly promising as new tool to characterize cardiac allograft rejection and to be complementary to EMB monitoring.

NARRATIVE ABSTRACT - Our study describes a method for detecting and characterising circulating extracellular vesicles (EV) as a minimally invasive, liquid biopsy for the diagnosis of cardiac allograft rejection, and as a complementary tool to EMB monitoring. EV obtained from peripheral blood were profiled to identify rejection and its types in cardiac transplant recipients. A standardized and rapid tool was established using a fluorescent bead-based multiplex assay. We built a diagnostic model based on machine learning algorithms to identify non-rejecting patients who potentially do not require EMBs. EV profiling could represent a tool for non-invasive monitoring of allograft rejection in cardiac transplant recipients.

Keywords: Extracellular Vesicles; Allograft Rejection; Heart Transplant; Biomarker; Machine Learning.

ABBREVIATION LIST: EMB, endomyocardial biopsy; ACR, acute cellular rejection; AMR, antibody-mediated rejection; EV, extracellular vesicles; NTA, nanoparticle tracking analysis; FC, flow cytometry; MFI, median fluorescence intensity; RF, random forest; DSA, donor-specific antibody.

INTRODUCTION

Allograft rejection remains a serious complication during and after the first post-transplant year(1, 2). More than 25% of patients have rejection episodes within one year and face the risk of developing consequent graft dysfunction with increased morbidity and mortality(3). Thus, early detection of cardiac allograft rejection is crucial to lower the risk of late morbidity and mortality. The current gold standard for diagnosis and grading of rejection is via endomyocardial biopsy (EMB). EMB is performed either to confirm clinical diagnosis of allograft rejection, or routinely in asymptomatic patients, as surveillance

monitoring for rejection(4, 5). EMB has also been used to evaluate efficacy of immunosuppression therapies in several clinical trials in which patients underwent more than 10 EMB during the first year after transplant(6, 7). This procedure still faces unresolved issues such as invasive risk, sampling error, and inter-reader variability(8-10). There is a long-standing effort toward the discovery of sensitive and noninvasive methods for the diagnosis of rejection that could be used in combination with tissue histology for reducing the frequency of biopsies(11). New, promising approaches are based on genomic screening, including microRNA(12, 13), and mRNA profiling(14). The non-invasive detection of circulating cell-free DNA (cfDNA)(15), or graft-derived cell-free DNA (GcfDNA)(16) were also proposed to diagnose acute cellular rejection (ACR), but not antibody-mediated rejection (AMR). Because nucleic acids and cell-free proteins are unstable in the circulation, a reliable quantification remains a critical problem.

Cells secrete extracellular vesicles (EV) that are composed of bioactive molecules mediating intercellular communication processes(17) and activating intracellular signalling pathways of target cells(18, 19). EV released into the circulation and body fluids display different RNA, protein, and lipid contents reflecting the homeostatic state and function of EV-producing cells. A change in the pathophysiological status of tissues and/or organs affects the composition of circulating EV, resulting in a specific molecular signature(20-22). This is of particular interest with regard to acute inflammatory processes, since EV have emerged as key regulators in immune responses(23-25). In this context, EV have great potential as diagnostic biomarkers in various diseases, including cardiovascular diseases(22) and might represent a valuable tool to support EMB in the diagnosis of different types of cardiac rejection. Given its limited invasiveness, the profiling of blood-derived EV represents an interesting diagnostic approach for monitoring early, post-transplant status and for therapeutic management of patients.

Here, we assessed, in a clinical setting, the potential of surface profiling of circulating EV for the diagnosis of acute cardiac allograft rejection, as companion biomarker to EMB monitoring. A multiplex

flow cytometric assay using antibody-coated capture beads was used to investigate differences in EV antigen expression in patients with an EMB diagnosis of ACR or AMR. Differentially expressed EV-surface antigens were combined in a single diagnostic model, based on machine learning algorithms, allowing for high accuracy discrimination between patients with and without graft rejection and among the different types of rejection. Finally, we validated our computational approach in an independent cohort of patients.

METHODS

A detailed description of patient data, EV isolation and characterization protocols, statistical analyses, and diagnostic modelling is provided in the Supplementary Appendix.

Patient selection and blood handling

Patients undergoing heart transplant were recruited at the Cardio-Surgery Center Gallucci (Dept. of Cardiac-Thoracic-Vascular Sciences and Public Health at the University Hospital of Padua, Italy). The study was approved by the local ethical committee and fully informed, written consent was provided by each patient. A total of 90 plasma samples were included and split into a training set (n=53) and a validation cohort (n=37). Patients with a first episode of rejection within 1 year since transplant were included in the study. Patients without rejection episodes within 1 year since transplant were enrolled as controls (Rejection 0, R0).

Patients from the training cohort were retrospectively selected between February 2018 and March 2019, including only subjects with an unequivocal diagnosis at EMB. According to the ISHLT classification for ACR, we selected EMBs showing 2R or 3A grade that correspond to multifocal inflammatory infiltrate, and multiple foci of myocyte necrosis. For AMR diagnosis, we selected EMBs corresponding to pAMR 1(I+) or pAMR 2, in presence of positivity for circulating donor specific antibodies.

For the validation cohort, we included 37 unselected consecutive patients, admitted for EBM between

April 2019 and January 2020, regardless of the final histologic diagnosis.

We excluded, from both validation and training cohorts, patients with other acute or chronic inflammatory disease (e.g., auto-immune disease, cancer, active infections).

All transplanted patients were ABO-compatible and were treated with cyclosporine, mycophenolate, and corticosteroids. All subjects enrolled in our study were scheduled for a surveillance biopsy in their regular follow-up after heart transplant in a setting of stable allograft function. Patients did not display any clinical signs/symptoms related to graft rejection (none of the patients was enrolled because rejection was suspected). Blood sampling was performed immediately before the EMB, thus avoiding potential confounding factors associated to procedure-related injury.

The diagnosis of either ACR or AMR was defined, according to the International Society for Heart and Lung Transplantation guidelines (4, 5) (see Supplementary Appendix).

Blood was collected in EDTA-treated tubes and centrifuged at 1,600 g for 15 minutes to separate plasma from cellular components; the low centrifuge speed avoided shear-stress-induced platelet activation. Plasma underwent serial centrifugation cycles to remove intact cells, cellular debris and larger EV: 3,000 g for 20 minutes, 10,000 g for 15 minutes, and 20,000 g for 30 minutes (Figure 1A). Cleared, platelet-free plasma was finally stored at -80°C and not thawed prior to analysis.

Plasma-derived EV quantification

Presence of specific EV markers and absence of apolipoprotein contaminants were assessed by western blotting. Size and concentration of plasma EV were determined by nanoparticle tracking analysis (NTA) using NanoSight LM10 (*Malvern Instruments, UK*) equipped with a 405 nm laser and Nanoparticle Tracking Analysis NTA 2.3 analytic software. EV concentration is shown as EV/mL (median value, interquartile range).

EV surface marker analysis by multiplex flow cytometry

All samples underwent bead-based EV immunocapture and were analyzed by flow cytometry (FC),

using MACSPlex human Exosome Kit (*Miltenyi Biotec, Germany*), according to manufacturer's instructions. Median fluorescence intensity (MFI) was measured on a MACSQuant Analyzer 10 flow cytometer according to previous validation studies(26-29). The multiplex platform analysis and gating strategy have previously been described(26, 28). MFI was evaluated for each subset of capture beads, corrected by subtracting the MFI of corresponding blank controls, and normalized by the mean MFI of CD9, CD63, and CD81.

Statistical analysis and diagnostic modelling

IBM SPSS Statistics 22 (IBM Corp., Armonk, New York, USA) and GraphPad PRISM 7.0a (La Jolla, California, USA) were used for statistical analyses. Scalar variables were analyzed with Kolmogorov–Smirnov test to evaluate distributions. Normally distributed variables are expressed as mean ± standard deviation and were analyzed by ANOVA with post-hoc Bonferroni's tests; non-normally distributed variables are expressed as median [interquartile range] and were analyzed by Kruskal-Wallis tests. Categorical variables are expressed as absolute number (percentage) and were compared with chi-square tests (Fisher's exact test when sample size was ≤ 5). Correlations were evaluated by Pearson's test (R coefficient) and analysis of regression curves. Receiver operating characteristics (ROC) curves were used to assess the area under the curve (AUC) and to compare diagnostic performances of selected variables; the Younden Index (J = sensitivity + specificity - 1) was calculated to assess the best sensitivity and specificity. *P*-values of less than 0.05 were considered significant.

Machine learning supervised algorithms are exploited in clinical practice to formulate predictions of selected outcomes based on a given set of labeled, paired, input-output training sample data(30, 31). To build the diagnostic model, a random forest (RF) algorithm was created using Python 3.5 (library, scikit-learn). The algorithm created 40 different classification trees; if at least 21 of 40 trees of the RF indicate the absence of rejection, the patient was classified as R0 (level 1); in case of detection of graft rejection, a second RF algorithm was created to distinguish ACR from AMR (level 2). A combined model was also

built to distinguish R0 *vs.* ACR *vs.* AMR, in a single step. Models were both internally and externally validated. Internal validation was provided by a leave-one-out cross-validation algorithm (see Supplementary Appendix). External validation was performed on an independent cohort enrolled in the same center.

Protein interactor network analysis

Protein interactors of the EV-surface marker were retrieved by Cytoscape PESCA plugin(32) and a global *Homo sapiens* protein-protein interaction (PPI) network of 1588 nodes and 36984 edges was reconstructed. For each quantitative comparison (R0 *vs.* ACR and R0 *vs.* AMR), a specific PPI sub-network per comparison was reconstructed considering the first neighbors of each differentially expressed EV-surface marker protein.

RESULTS

Patient characteristics

We enrolled 90 subjects, 53 in the training cohort and 37 in the validation cohort. Patient characteristics are summarized in Tables 1, S1, and S2. All subjects enrolled were scheduled for a surveillance biopsy in their regular follow-up in a setting of stable allograft function.

According to EMB parameters and biochemical analyses, patients from training cohort were divided in three groups (R0, ACR, AMR). They were similar with respect to sex and age, whereas the time from heart transplant to rejection was 3 [2;8] months for the ACR group compared to 11 [9;14] months for the AMR group (P=0.004). Among AMR patients, 4 of 9 (44.4%) presented with capillary deposition of complement fraction C4d, and 2 of 9 (22.2%), with CD68-positive staining in macrophages with a grading >10%. The anti-HLA antibody assessment revealed all AMR patients as positive for anti-HLA-II donor-specific antibodies (DSA) and anti-HLAII non-DSA. Moreover, 8 of 9 (88.9%) patients in the AMR group displayed a strong positivity for anti-HLA-I non-DSA. As expected, the cellular rejection

score was higher in patients with ACR compared to both controls and AMR patients. Biochemical parameters and the ejection fraction at echocardiography are reported in Table S2. For diagnostic modelling purpose, an independent cohort was enrolled. Clinical, biochemical, and EMB parameters did not significantly differ from the training cohort (Table S3).

EV quantification

The immunocapture assay was validated for its specificity to bind vesicles by western blotting analysis for the presence of specific EV markers such as TSG101 and CD81 and for the absence of contaminants such as apolipoprotein (ApoB48; Figure 1B). Given the reliability of the immunocapture protocol, we used the level of expression of tetraspanins CD9, CD63, and CD81 (generally accepted EV surface markers) for specific quantification of circulating EV. The MFI of tetraspanins was higher in patients with ACR and AMR, compared to R0 (P<0.001; Figure 1C and Table S4).

Size and concentration profiles of circulating EV were determined by NTA. NTA confirmed a significant increase of the concentration of plasma-derived EV in patients undergoing rejection compared to subjects classified as R0; no differences were observed between ACR and AMR (Figure S1A and Table S4). Overall, the increase in the total number of EV reflects a concentration of the smaller subset (30-150 nm) that was approximately three-fold higher in ACR and AMR compared to R0 (P<0.01 for both comparisons; Figure S1A). Consistently, the median EV diameter was significantly lower in ACR and AMR *vs.* R0 (P<0.001; Figure S1B and Table S4). Cumulative distribution plots (EV concentration *vs.* particle size), resulted in a left-shift of curves and higher AUC for ACR and AMR as compared to R0 (P<0.001 for both; Figure 1D). Although NTA cannot distinguish EV from other particles such as lipoproteins, the analysis correlates with the antigenic quantification of CD9/CD63/CD81 (Pearson's R=0.463; P<0.001; Figure 1E).

Analysis of EV-surface markers

Immunocaptured EV from pre-cleared plasma of patients from the training cohort (n=53) were analyzed for the expression of 37 different surface antigens (Table S5). Several biomarkers were significantly higher in both ACR and AMR patients compared to R0 (Figure 2A). This applied for four antigens including the molecules of major histocompatibility complex class-I (HLA-I), the platelet membrane glycoprotein II-b (CD41b) and two non-immune system-related antigens: tyrosine-protein kinase transmembrane receptor (ROR1) and Stage-Specific Embryonic Antigen-4 (SSEA-4). Expression levels of two T-cell surface antigens, CD2 and CD3, that function as a cell adhesion molecule and a co-receptor activator, respectively, were differentially expressed between ACR patients *vs.* R0. In addition, the surface EV expression of five, well-established, immunologic markers was significantly higher in AMR patients as compared to R0: major histocompatibility complex class II (HLA-II), the epithelial cell adhesion molecule (CD326), B-lymphocyte antigens CD19 and CD20 and the interleukin-2 receptor alpha chain (CD25). Compared to R0, the heatmap highlights clusters corresponding to high MFI for CD2, CD3, ROR1, SSEA-4, HLA-I and CD41b in ACR patients, and to high ROR1, SSEA-4, HLA-I, CD41b, HLA-II, CD326, CD19, CD25, and CD20 in AMR patients (Figure 2B).

Diagnostic Modelling

The power of discrimination between patients presenting graft rejection and non-rejecting R0 controls was evaluated by analysis of ROC curves for each single, differentially expressed EV-surface marker. Overall, the MFI analysis displayed a reliable diagnostic performance for all the evaluated markers (Figure 3). Comparing ACR *vs.* R0, the best performance was obtained for HLA-I (AUC 0.939), CD3 (AUC 0.848) and SSEA-4 (AUC 0.832), CD2 (AUC 0.829). Of note, the MFI for EV-carried HLA-I, CD2 and SSEA-4 displayed a sensitivity of 100% in the diagnosis of ACR, with specificities ranging between 63.6 and 87.9% (Figure 3A, and 3C). For AMR *vs.* R0, ROR1 showed the best performance with an AUC of 0.879 (sensitivity and specificity of 100% and 75.8%, respectively), followed by HLA-I (AUC 0.872), SSEA-4 (AUC 0.820), CD20 (AUC 0.798), CD19 (AUC 0.795), HLA-II (AUC 0.788),

and CD41b (AUC 0.778). Strengthening our results, ROR1, SSEA-4, HLA-II and CD41b each achieved 100% sensitivity, correctly identifying all patients with AMR (Figure 3B, and 3D).

After having demonstrated excellent diagnostic performances for each candidate biomarker considered individually, we combined the 11 differentially expressed EV-surface antigens in a single diagnostic model using machine learning algorithms. A RF classification model was used as computational approach to identify patients with heart rejection using the MFI of circulating EV-carried antigens (Figure 4). The RF model was developed in the training cohort (n=53) and then internally validated by a leave-one-out cross-validation algorithm (see methods), which simulated how the model could generalize on an independent cohort. Finally, we performed a real external validation of the RF model on an independent cohort enrolled in the same center.

At the training, a double level RF model was built as a first approach: the first level discriminated the presence of rejection (including both ACR and AMR) *vs.* no-rejection (R0) with an accuracy of 100%. All identified rejecting subjects (n=20), were then introduced in the second level, to distinguish between the two rejection types (ACR *vs.* AMR); this second model also provided a very high performance with an accuracy of 95%. All patients except one were correctly identified; a single patient with AMR was classified as ACR (Figure 4A). Next, we built a combined model to classify patients in one single step (R0 *vs.* ACR *vs.* AMR); all subjects were correctly allocated with an accuracy of 100% (Figure 4B). We then provided an internal validation by a leave-one-out cross-validation algorithm to simulate how the algorithms could perform in an independent cohort and to exclude overfitting bias (effect due to the best performance of the model in the cohort in which it is trained). The accuracy was still very high (83% to 88.7%), with a modest overfitting effect (11.3% to 17%). Finally, we tested our model in an independent external validation cohort (Figure 5). Consistently with the internal validation, the accuracy was 86.5%, 81.3%, and 78.4%, respectively for level 1, level 2, and combined RF models, thus confirming a reliable diagnostic performance even in an external cohort of patients.

The enrollment of consecutive unselected patients in the validation cohort, allowed us to simulate a clinical context in which EV profiling and random forest model were integrated not to avoid EMBs, but to select patients for this procedure. With this approach, we would have correctly managed 34 of 37 patients (accuracy 91.9%), while reducing by 56.8% the number of EMBs required (Figure 6). Unfortunately, 3 rejecting patients would have been predicted as R0, thus missing the possibility to be correctly managed by EMBs.

Correlation analyses

Patients from training and validation cohorts were pooled and correlation analyses were performed to evaluate whether expression levels of EV-surface markers and EV concentration might relate to EMB findings and/or patient characteristics. Cellular rejection score correlates with EV concentration and with the expression level of SSEA-4, HLA-I, CD41b (R range 0.323-0.581, $P<0.01$) in patients with ACR. Significant correlations have been also found between circulating levels of anti-HLA-I (DSA and non-DSA), and anti-HLA-II (DSA and non-DSA) antibodies and EV concentration, or MFI of ROR1 and HLA-I (R range 0.253-0.465, $P<0.05$; Table S6) in patients with AMR.

Moreover, a significant correlation was found between lymphocyte counts and EV concentration. The number of lymphocytes and/or monocytes were also correlated to expression levels of HLA-II, CD25, HLA-I, SSEA-4, and CD41b in AMR and R0 patients, and to the expression of CD2, SSEA-4, and CD41b in ACR and R0 patients (Table S7). No significant correlations were observed between EV-surface markers and age at heart transplant, or time to rejection onset.

A sub-analysis aiming to assess the sex-specific expression of EV surface antigens demonstrated a selective over-expression of CD3, CD19, CD2, CD25, and CD20 in rejecting females, whereas CD41b was over-expressed in male rejecting patients. In addition, the increase in EV concentration assessed by CD9/CD63/CD81 MFI was more relevant in female patients with rejection, as compared to males (Table S8). Finally, we performed a correlation analysis between EMB findings and the expression of EV

markers. CD3, ROR1, SSEA-4, HLA-I, and CD41b MFI were directly correlated to the presence of inflammatory infiltrate, myocytolisis, myocyte necrosis, and/or vasculitis in ACR patients (R range 0.239-0.513, $P<0.05$). HLA-II, SSEA-4, and HLA-I were correlated to the presence of inflammatory infiltrate and vasculitis in AMR patients (R range 0.238-0.462, $P<0.05$; Table S9).

Protein interactor network analysis

Since secreted EV have been shown to mediate autocrine, paracrine and endocrine signaling, we performed a theoretical analysis to predict possible protein-protein interactors. The network analysis allowed identification of potential protein targets, biological pathways and molecular functions that could be affected by EV-surface markers that were differentially expressed in rejecting vs. not rejecting patients. "Hubs" and "bottlenecks" refer to proteins with greater numbers of protein connections or to those occupying critical network positions, suggesting pivotal roles for the management of information flow over the network (33) (Figure S1);. Except for HLA-E, hubs and bottlenecks in the interactor networks for ACR and AMR were different: ABI1, CD247, ERBB3, JUN, and B2M were identified as main interactors in ACR, whereas CD74, VAPA, SSR4, COPB1, PTCH1, DYNLL1, SGTA, RANBP9, and ITGA6 were main interactors in AMR (Tables S10, and S11). The higher number of EV-marker interactors in both ACR and AMR networks led to the enrichment of specific pathways related to the immune system and signal transduction, involving the inflammatory response, intercellular communication, cell survival, and apoptosis.

DISCUSSION

The present study highlights the diagnostic potential of circulating EV as biomarkers for monitoring cardiac allograft rejection. We found that the total amount of circulating vesicles assessed by the expression of specific surface antigens CD63, CD81, and CD9, discriminated between patients with and without rejection. Both ACR and AMR patients showed an increase in EV concentration, compared to

R0. Nanoparticle tracking analysis (NTA), which strongly correlated with the expression of tetraspanins (CD63, CD9 and CD81), showed an increase in EV concentration for rejecting patients, specifically for small-sized EVs (≤150 nm, the size specifically associated with exosomes). These results are consistent with the notion that the inflammatory state induces the release of microvesicles (34). Most importantly, plasma-derived EV carry a specific set of surface antigens, reflecting the change in immunologic profile of heart transplant recipients. The level of expression of specific, membrane-associated markers significantly diverged in patients with no rejection from those with rejection, and above all, different types of rejection were discriminated by EV profiling. Eleven of 37 analyzed surface antigens were differentially expressed in patients with ACR and AMR compared to patients without rejection. Six markers identified a cluster of patients with ACR, whereas nine markers identified patients with AMR. Finally, ROC curves revealed high performances for the evaluated EV markers, with 100% sensitivity reached for several markers (HLA-I, CD2 and SSEA-4 for ACR; ROR1, SSEA-4, HLA-II and CD41b for AMR). The diagnostic potential was further improved by combining MFI values of the 11 EV surface antigens differentially expressed between groups through a machine learning approach.

The accuracy of our computational approach resulted in a theoretical validation of ~89% and it stands at ~87% when the validation was performed on a separate cohort of patients, with a negligible overfitting effect of about 2%.

In light of what stated above, the immuno-profiling of plasma-derived EV and the integration of complex computational approaches in the management of patients after heart transplant, would help clinicians to discriminate between patients requiring EMB from those who may not require this procedure.

The major strength of EV profiling approach is that it resulted in a consistent (it has been validated on patients) and reliable (with a relevant diagnostic performance) non-invasive diagnostic test, that can eventually reduce the number of biopsies for non-rejecting patients. By using the proposed model to simulate the management of subjects included in the validation cohort (37 consecutively enrolled

patients), introducing blood sampling and EV analysis before the EMB procedure, we could have reduced the number of patients selected for biopsy by 56.8% (flowchart in Figure 6). Unfortunately, three rejecting patients would have missed the possibility to be correctly managed through EMB.

Another strength that should be considered in envisioning the profiling of EV as potential diagnostic tool lies in the fact that by analyzing systemic circulating particles, clinicians can quickly grasp a more complete picture of patient's status. Indeed, differentially expressed markers on the surface of EV in blood may be more representative as compared to markers detected in tissue sample, which can be distorted by necrosis and fibrotic areas. Although, we did not select cardiac specific EV, as to date there is no specific antibody recognizing tissue specific vesicles, EV in blood presumably includes particles released from injured areas of tissue, but preferentially exclude necrotic areas in which circulation has ceased.

Other studies have evaluated profiling of circulating EV to non-invasively monitor cardiac allografts for rejection. Kennel et al. performed proteomic analysis by liquid chromatography-tandem mass spectrometry on serum-derived exosomes (small EV) collected from heart transplant recipients with no rejection, ACR, and AMR(35). They found that allograft rejection alters the protein content of circulating exosomes, giving them unique protein expression patterns, which are suitable as predictive and prognostic biomarkers. Although very interesting, the approach used by Kennel at al. was based on relatively complex methodologies and instrumentation. Here we propose the profiling of the surface of EV which does not require lysis or digestion steps and can be performed using conventional flow cytometers. Habertheuer et al. have recently shown that transplanted hearts release donor-specific exosomes. In a murine model of heterotopic heart transplant, they elegantly showed that the cardiac allograft releases a distinct pool of donor MHC-specific exosomes into recipient circulation. The signal peaked during early stages of acute rejection with high accuracy(36) enabling the development of a very specific and sensitive biomarker platform for allograft monitoring (36, 37). Compared to this study that

was carried out in a model of major histocompatibility mismatch using immunodeficient recipient mice, our platform has been analyzed in a clinical setting, including immunocompetent recipients on maintenance immuno-suppression, and provides comparable accuracy.

Quantitative changes in microRNA cargo of serum exosomes from heart transplant recipients has also been demonstrated. Dewi and colleagues showed that microRNA miR-142-3p increased in case of ACR(38). miR-142-3p is enclosed into secreted exosomes from T cells and targets specific messenger RNA in endothelial cells, thus implying a role for T cell-derived EV in mediating graft rejection[38]. In line with this hypothesis, we found that CD3 and CD2, T cell co-receptors, were both upregulated on the surface of EV in patients with a diagnosis of ACR. It might be interesting, in the future, to assess whether the EV expressing these surface co-receptors also carry miR-142-3p. This scenario would reinforce the role of the endothelial-T cells axis in cell-mediated rejection.

EV surface antigens may also reflect activation of B-cells. The receptor tyrosine kinase ROR1, which is a transmembrane protein highly expressed on the surface of leukemia cells, but not on normal B-cells(39)·(40), was significantly overexpressed in both AMR and ACR patients as compared to controls. However, none of the patients with rejection displayed proliferative hematologic disorders, thus ROR1 expression on EV might reflect an activation state of B-cells, which is not associated with a malignant phenotype. Given the correlation with clinical, biochemical, and EMB parameters we found significantly correlated between EV-surface markers and the numbers of circulating lymphocytes and monocytes in rejecting patients. The total number of WBCs was not increased in patients with a diagnosis of rejection, suggesting that EV number and profile may reflect the activation state of these cells and the systemic inflammatory response in transplant rejection(41). EV surface markers were also correlated with the presence of inflammatory infiltrate, myocytolisis, myocyte necrosis, and vasculitis on EMB, being associated not only to the diagnosis of ACR/AMR, but also to the severity of the inflammatory response triggered by rejection.

Although beyond the scope of the present paper, we hypothesized that EV antigens may exert active biological functions providing autocrine and paracrine signals to target cells (19, 42)·(43). In this regard, we performed a theoretical interactor network analysis which suggested that the large majority of proteins up-regulated on EV of rejecting patients may have a potential role as ligand–receptor interactors for several intercellular pathways involved in the inflammatory response to graft rejection. For instance, circulating EV can act as extracellular stimuli for Jun (hub/bottleneck in ACR network), which controls a number of cellular processes including differentiation, proliferation, and apoptosis through the formation of heterodimer AP-1(44). This carries importance when considering that allograft treatment with decoy oligodeoxynucleotides (ODN) targeting the transcription factor AP-1 delays acute rejection and prolongs cardiac allograft survival in a rat transplant model(45). Interestingly, the network analysis highlighted a possible EV-mediated induction of genes related to natural killer (NK) cells and these findings are in line with recent tissue-based gene profiling unveiling the association of NK transcripts with chronic allograft vasculopathy in AMR (46).

After stratification for sex, we found several EV markers selectively enriched in female rejecting patients. In particular, the overexpression of surface antigens CD19 and CD 20 (both markers of B-cells) is noteworthy, as it is known that estrogens amplify immuno-responses in women (47, 48). They act by increasing total number of progenitor B cells (49), and inducing B cell activation (50).

The main limit of the present study is that the patients used for training and validation of the model did not allow us for longitudinal-based cohort study, thus limiting the evaluation of our model as predictive approach. Indeed, a longitudinal cohort would have allowed the demonstration of whether this approach may identify rejection before the diagnosis made by EMB, and whether changes in EV related parameters may even anticipate the histologic evidence of rejection, thus enabling the institution of an earlier and perhaps less intrusive treatment. A second important issue is the absence of specific, cardiac-derived antigens among the EV markers included in the analysis, thus excluding the possibility of grading the

vascular damage and cardiac damage related to rejection. Another potential limitation is the relatively small sample size. Our selection strategy at training was based on a well-defined histological pattern at EMB (see methods). This allowed us to evaluate highly selected patients and train the diagnostic model on subjects that truly underwent rejection. On the other hand, this can be a limitation as the training of the model does not include subjects with mild forms of rejection. However, the validation of the model was performed on an unselected cohort of patients, thus suggesting a potential clinical application, even if the present findings still have to be confirmed in larger prospective cohorts. Finally, we showed that different types of rejection are associated with different EV phenotypes, but we cannot define whether these phenotypes are specific for rejection, as the large majority of antigens might be theoretical associated with other acute and chronic inflammatory diseases.

In conclusion, given its low cost, speed, and simplicity, as well as its high accuracy, the method here described provides a connection between allograft phenotypes, biochemical indexes, and histology parameters for the detection of different types of heart allograft rejection. Circulating plasma-derived EV are a highly promising tool for characterising and monitoring cardiac allograft rejection. It does not standalone as diagnostic biomarker that could completely replace EMB. The quantitative flow cytometer analysis and the computational approach proposed here can act in synergy with tissue histology and offer a tool to clinician for reducing the number of biopsies and selecting patients with the highest risk of rejection for a closer follow-up.

ACKNOWLEDGMENTS - All authors contributed extensively to the work presented in this manuscript. L.B., and A.A. designed the study. C.C., F.T., T.B., G.G., and M.F. recruited patients and collected clinical information and blood samples. J.B., C.C., V.B., and S.B., performed the EV isolation and characterization. J.B., A.B., and D.D.S. performed statistics, diagnostic modelling, and protein interactor network analysis. J.B., C.C., A.A., and L.B. wrote the manuscript with inputs from all authors. S.L.L., G.T., C.B., G.V., L.B., and A.A. interpreted data and critically revised the manuscript.

Source(s) of Funding: This study was supported by research grant from University of Padua BIRD170215, BIRD199570 and by the Registry of Cardio-Cerebral-Vascular Pathology, Veneto Region, Italy. L.B. and S.L. were supported by research grant of Swiss National Science Foundation (IZCOZ0_182948/1), Switzerland. L.B. was supported by research grant of Velux Stiftung, Zurich (Switzerland). This article is based upon work from COST Action EU-CARDIOPROTECTION CA16225 supported by COST (European Cooperation in Science and Technology).

Conflict(s) of Interest/Disclosure(s): nothing to disclose.

REFERENCES

1. Yusen RD, Edwards LB, Dipchand AI, et al.: The Registry of the International Society for Heart and Lung Transplantation: Thirty-third Adult Lung and Heart-Lung Transplant Report-2016; Focus Theme: Primary Diagnostic Indications for Transplant. J Heart Lung Transplant 2016;35:1170-84.
2. Weber BN, Kobashigawa JA, Givertz MM: Evolving Areas in Heart Transplantation. JACC Heart Fail 2017;5:869-78.
3. Lund LH, Edwards LB, Kucheryavaya AY, et al.: The registry of the International Society for Heart and Lung Transplantation: thirty-first official adult heart transplant report--2014; focus theme: retransplantation. J Heart Lung Transplant 2014;33:996-1008.
4. Stewart S, Winters GL, Fishbein MC, et al.: Revision of the 1990 working formulation for the standardization of nomenclature in the diagnosis of heart rejection. J Heart Lung Transplant 2005;24:1710-20.
5. Berry GJ, Burke MM, Andersen C, et al.: The 2013 International Society for Heart and Lung Transplantation Working Formulation for the standardization of nomenclature in the pathologic diagnosis of antibody-mediated rejection in heart transplantation. J Heart Lung Transplant 2013;32:1147-62.
6. Hershberger RE, Starling RC, Eisen HJ, et al.: Daclizumab to prevent rejection after cardiac transplantation. N Engl J Med 2005;352:2705-13.
7. Grimm M, Rinaldi M, Yonan NA, et al.: Superior prevention of acute rejection by tacrolimus vs. cyclosporine in heart transplant recipients--a large European trial. Am J Transplant 2006;6:1387-97.
8. Wong RC, Abrahams Z, Hanna M, et al.: Tricuspid regurgitation after cardiac transplantation: an old problem revisited. J Heart Lung Transplant 2008;27:247-52.
9. Nguyen V, Cantarovich M, Cecere R, Giannetti N: Tricuspid regurgitation after cardiac transplantation: how many biopsies are too many? J Heart Lung Transplant 2005;24:S227-31.

10. Bishawi M, Zanotti G, Shaw L, et al.: Tricuspid Valve Regurgitation Immediately After Heart Transplant and Long-Term Outcomes. Ann Thorac Surg 2019;107:1348-55.
11. Hamour IM, Burke MM, Bell AD, Panicker MG, Banerjee R, Banner NR: Limited utility of endomyocardial biopsy in the first year after heart transplantation. Transplantation 2008;85:969-74.
12. Di Francesco A, Fedrigo M, Santovito D, et al.: MicroRNA signatures in cardiac biopsies and detection of allograft rejection. J Heart Lung Transplant 2018;37:1329-40.
13. Duong Van Huyen JP, Tible M, Gay A, et al.: MicroRNAs as non-invasive biomarkers of heart transplant rejection. Eur Heart J 2014;35:3194-202.
14. Halloran PF, Potena L, Van Huyen JD, et al.: Building a tissue-based molecular diagnostic system in heart transplant rejection: The heart Molecular Microscope Diagnostic (MMDx) System. J Heart Lung Transplant 2017;36:1192-200.
15. De Vlaminck I, Valantine HA, Snyder TM, et al.: Circulating cell-free DNA enables noninvasive diagnosis of heart transplant rejection. Sci Transl Med 2014;6:241ra77.
16. Beck J, Oellerich M, Schulz U, et al.: Donor-Derived Cell-Free DNA Is a Novel Universal Biomarker for Allograft Rejection in Solid Organ Transplantation. Transplant Proc 2015;47:2400-3.
17. Maas SLN, Breakefield XO, Weaver AM: Extracellular Vesicles: Unique Intercellular Delivery Vehicles. Trends Cell Biol 2017;27:172-88.
18. S ELA, Mager I, Breakefield XO, Wood MJ: Extracellular vesicles: biology and emerging therapeutic opportunities. Nat Rev Drug Discov 2013;12:347-57.
19. Cervio E, Barile L, Moccetti T, Vassalli G: Exosomes for Intramyocardial Intercellular Communication. Stem Cells Int 2015;2015:482171.

20. Pant S, Hilton H, Burczynski ME: The multifaceted exosome: biogenesis, role in normal and aberrant cellular function, and frontiers for pharmacological and biomarker opportunities. Biochem Pharmacol 2012;83:1484-94.
21. Revenfeld AL, Baek R, Nielsen MH, Stensballe A, Varming K, Jorgensen M: Diagnostic and prognostic potential of extracellular vesicles in peripheral blood. Clin Ther 2014;36:830-46.
22. Barile L, Vassalli G: Exosomes: Therapy delivery tools and biomarkers of diseases. Pharmacology & therapeutics 2017;174:63-78.
23. Boulanger CM, Loyer X, Rautou PE, Amabile N: Extracellular vesicles in coronary artery disease. Nat Rev Cardiol 2017;14:259-72.
24. Haller PM, Stojkovic S, Piackova E, et al.: The association of P2Y12 inhibitors with pro-coagulatory extracellular vesicles and microRNAs in stable coronary artery disease. Platelets 2019:1-8.
25. Sarkar A, Mitra S, Mehta S, Raices R, Wewers MD: Monocyte derived microvesicles deliver a cell death message via encapsulated caspase-1. PLoS One 2009;4:e7140.
26. Wiklander OPB, Bostancioglu RB, Welsh JA, et al.: Systematic Methodological Evaluation of a Multiplex Bead-Based Flow Cytometry Assay for Detection of Extracellular Vesicle Surface Signatures. Front Immunol 2018;9:1326.
27. El Andaloussi S, Lakhal S, Mager I, Wood MJ: Exosomes for targeted siRNA delivery across biological barriers. Adv Drug Deliv Rev 2013;65:391-7.
28. Koliha N, Wiencek Y, Heider U, et al.: A novel multiplex bead-based platform highlights the diversity of extracellular vesicles. J Extracell Vesicles 2016;5:29975.
29. Andriolo G, Provasi E, Lo Cicero V, et al.: Exosomes From Human Cardiac Progenitor Cells for Therapeutic Applications: Development of a GMP-Grade Manufacturing Method. Frontiers in Physiology 2018;9.

30. Burrello J, Burrello A, Stowasser M, et al.: The Primary Aldosteronism Surgical Outcome Score for the Prediction of Clinical Outcomes After Adrenalectomy for Unilateral Primary Aldosteronism. Ann Surg 2019.
31. Meyer LS, Wang X, Susnik E, et al.: Immunohistopathology and Steroid Profiles Associated With Biochemical Outcomes After Adrenalectomy for Unilateral Primary Aldosteronism. Hypertension 2018;72:650-7.
32. Scardoni G, Tosadori G, Pratap S, Spoto F, Laudanna C: Finding the shortest path with PesCa: a tool for network reconstruction. F1000Res 2015;4:484.
33. Vella D, Zoppis I, Mauri G, Mauri P, Di Silvestre D: From protein-protein interactions to protein co-expression networks: a new perspective to evaluate large-scale proteomic data. EURASIP J Bioinform Syst Biol 2017;2017:6.
34. Puddu P, Puddu GM, Cravero E, Muscari S, Muscari A: The involvement of circulating microparticles in inflammation, coagulation and cardiovascular diseases. Can J Cardiol 2010;26:140-5.
35. Kennel PJ, Saha A, Maldonado DA, et al.: Serum exosomal protein profiling for the non-invasive detection of cardiac allograft rejection. J Heart Lung Transplant 2018;37:409-17.
36. Habertheuer A, Korutla L, Rostami S, et al.: Donor tissue-specific exosome profiling enables noninvasive monitoring of acute rejection in mouse allogeneic heart transplantation. J Thorac Cardiovasc Surg 2018;155:2479-89.
37. Vallabhajosyula P, Korutla L, Habertheuer A, et al.: Tissue-specific exosome biomarkers for noninvasively monitoring immunologic rejection of transplanted tissue. J Clin Invest 2017;127:1375-91.

38. Sukma Dewi I, Celik S, Karlsson A, et al.: Exosomal miR-142-3p is increased during cardiac allograft rejection and augments vascular permeability through down-regulation of endothelial RAB11FIP2 expression. Cardiovasc Res 2017;113:440-52.
39. Choi MY, Widhopf GF, 2nd, Wu CC, et al.: Pre-clinical Specificity and Safety of UC-961, a First-In-Class Monoclonal Antibody Targeting ROR1. Clin Lymphoma Myeloma Leuk 2015;15 Suppl:S167-9.
40. Saleh RR, Antras JF, Peinado P, et al.: Prognostic value of receptor tyrosine kinase-like orphan receptor (ROR) family in cancer: A meta-analysis. Cancer Treat Rev 2019;77:11-9.
41. Burrello J, Monticone S, Gai C, Gomez Y, Kholia S, Camussi G: Stem Cell-Derived Extracellular Vesicles and Immune-Modulation. Front Cell Dev Biol 2016;4:83.
42. Margolis L, Sadovsky Y: The biology of extracellular vesicles: The known unknowns. PLoS Biol 2019;17:e3000363.
43. Segura E, Amigorena S, Thery C: Mature dendritic cells secrete exosomes with strong ability to induce antigen-specific effector immune responses. Blood Cells Mol Dis 2005;35:89-93.
44. Ameyar M, Wisniewska M, Weitzman JB: A role for AP-1 in apoptosis: the case for and against. Biochimie 2003;85:747-52.
45. Holschermann H, Stadlbauer TH, Wagner AH, et al.: STAT-1 and AP-1 decoy oligonucleotide therapy delays acute rejection and prolongs cardiac allograft survival. Cardiovasc Res 2006;71:527-36.
46. Loupy A, Duong Van Huyen JP, Hidalgo L, et al.: Gene Expression Profiling for the Identification and Classification of Antibody-Mediated Heart Rejection. Circulation 2017;135:917-35.
47. Khan D, Ansar Ahmed S: The Immune System Is a Natural Target for Estrogen Action: Opposing Effects of Estrogen in Two Prototypical Autoimmune Diseases. Front Immunol 2015;6:635.

48. Morgan AE, Dewey E, Mudd JO, et al.: The role of estrogen, immune function and aging in heart transplant outcomes. Am J Surg 2019;218:737-43.
49. Bouman A, Heineman MJ, Faas MM: Sex hormones and the immune response in humans. Hum Reprod Update 2005;11:411-23.
50. Ansar Ahmed S, Penhale WJ, Talal N: Sex hormones, immune responses, and autoimmune diseases. Mechanisms of sex hormone action. Am J Pathol 1985;121:531-51.

TABLE LEGENDS

Table 1 –**Characteristics of patients from the training cohort.** Sex, age at heart transplant (HT), endomyocardial biopsy (EMB) characteristics, cellular rejection score (RS) and HLA-I/II donor- specific and nonspecific antibodies (DSA) in patients from the training cohort, without rejection (R0; n=33), with cellular-mediated (ACR; n=11) or with antibody-mediated rejection (AMR; n=9). *P*-values of less than 0.05 were considered significant (in bold).

FIGURE LEGENDS

Figure 1 – **EV characterization.** Characterization of circulating extracellular vesicles (EV) from patients of the training cohort with cellular-mediated rejection (ACR; orange; n=11), antibody-mediated rejection (AMR blue; n=9), compared to controls without graft rejection (rejection 0, R0; green; n=33). (A) Patient samples underwent serial centrifugation and then EV were characterized by nanoparticle tracking analysis (NTA) and standardized multiplex flow cytometry for the evaluation of 37 different EV surface antigens. (B) Western blot analysis of plasma and EV isolated by bead immuno-capture (n=4) for 2 EV markers (TSG101 and CD81) and a potential contaminant (Apolipoprotein, B48). (C) Median fluorescence intensity (MFI, %) of CD9, CD63, and CD81 by flow cytometric analysis. (D) Cumulative distribution plot combining EV concentration (n/mL; y axis) and diameter (nm; x axis). (E) Correlation between EV concentration and CD9-CD63-CD81 MFI. The regression line is depicted in red, with a 95% confidence interval. Data are expressed as median and interquartile range (panel C). *P* values < 0.05 were considered significant (*$P < 0.05$; **$P < 0.01$).

Figure 2 – **EV-surface markers.** Median fluorescence intensity (MFI, expressed as a percentage [%], after normalization with mean MFI of CD9, CD63, and CD81) for differentially expressed EV surface markers in patients with cellular-mediated rejection (ACR; orange; n=11), antibody-mediated rejection

(AMR; blue; n=9), or without graft rejection (rejection 0, R0; green; n=33). (A) EV surface markers were divided into three groups in which EV markers were significantly increased: in patients with ACR *vs.* R0 (left), in patients with AMR *vs.* R0 (right), and both rejection groups *vs.* R0 (middle). Patients with ACR are represented in orange (n=11), AMR in blue (n=9), and the R0 group in green (n=33). Horizontal lines on the circles indicate significant increases compared to R0 ($P < 0.05$). (B) Heat map representing EV surface marker expression in patients stratified for diagnosis (red, low fluorescence; green, high fluorescence)..

Figure 3 – **Diagnostic performances of EV surface markers.** Diagnostic performances of EV surface markers differentially expressed in patients without rejection (R0) compared to cellular-mediated rejection (ACR; n=44; panels A and C) and antibody-mediated rejection (AMR; n=42; panels B and D). The area under the curve (AUC), asymptotic difference compared to the referral line (dashed grey line), sensitivity, and specificity are reported for each marker.

Figure 4 – **Diagnostic Modelling.** Random forest (RF) model for the diagnosis of allograft rejection using MFI values for the 11 EV surface markers differentially expressed among patients with cellular-mediated rejection (ACR; orange; n=11), antibody-mediated rejection (AMR blue; n=9), compared to controls without graft rejection (rejection 0, R0; green; n=33). (A) Double level RF model. Level 1 identifies patients with graft rejection, whereas Level 2 distinguishes between AMR and ACR. (B) Combined model discriminating between R0, ACR, and AMR in a single step. Representative classification trees and confusion matrix at training and internal validation of the model are reported for each model. The sole missing patient with rejection is highlighted in red.

Figure 5 – **External validation of random forest diagnostic models**. The random forest models (level 1, level 2, and the combined model) were validated on an independent external cohort (n=37). (A) Heat map representing EV surface marker expression in patients from the external validation cohort (n=37): acute cellular rejection (ACR; orange; n=13), antibody-mediated rejection (AMR; blue; n=4), or without graft rejection (rejection 0, R0; green; n=20). (B, C, and D) Confusion matrix reporting accuracy, real, and predicted diagnosis, are reported for each model. Missed rejecting patients are underlined in red.

Figure 6 – **Simulated application of EV profiling in clinical practice.** The random forest model (level 1) was applicated to the validation cohort (n=37) to select patients for endomyocardial biopsy (EMB) (A) Management of heart transplanted patients using EMB as gold standard; all patients are correctly managed (accuracy 100%; number of EMB = 37). (B) Flow chart integrating EV profiling in patient management; 34 of 37 patients would be correctly managed (accuracy 91.9%; number of EMB = 16 [-56.8%]); 3 patients (in red) were misclassified and would miss the possibility to performed EMB.

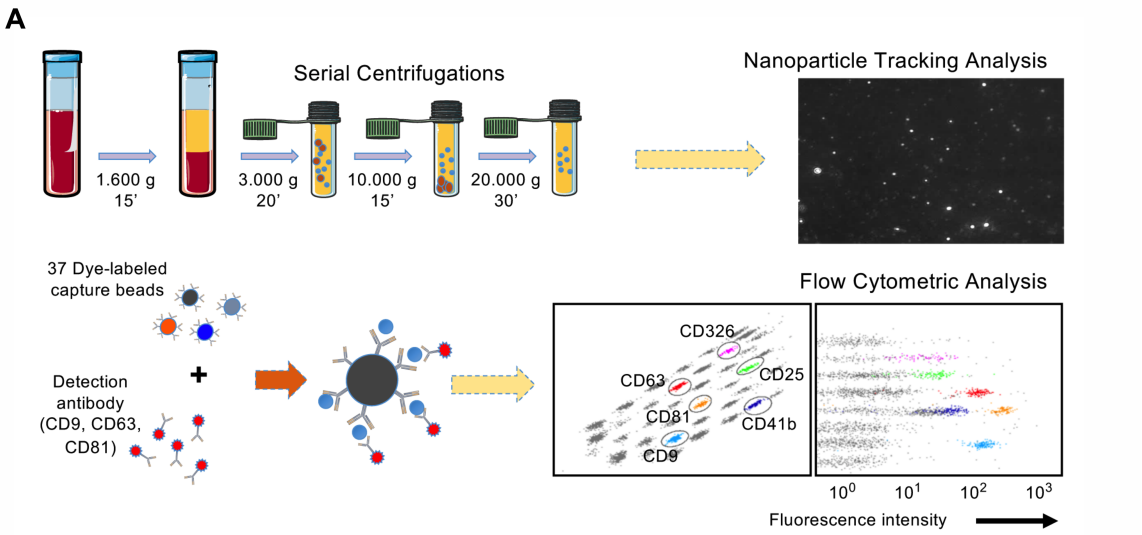
A
Serial Centrifugations
1.600 g
15'
3.000 g
20'
10.000 g
15'
20.000 g
30'
Nanoparticle Tracking Analysis
37 Dye-labeled capture beads
Detection antibody (CD9, CD63, CD81)
Flow Cytometric Analysis
CD326
CD25
CD63
CD81
CD41b
CD9
Fluorescence intensity

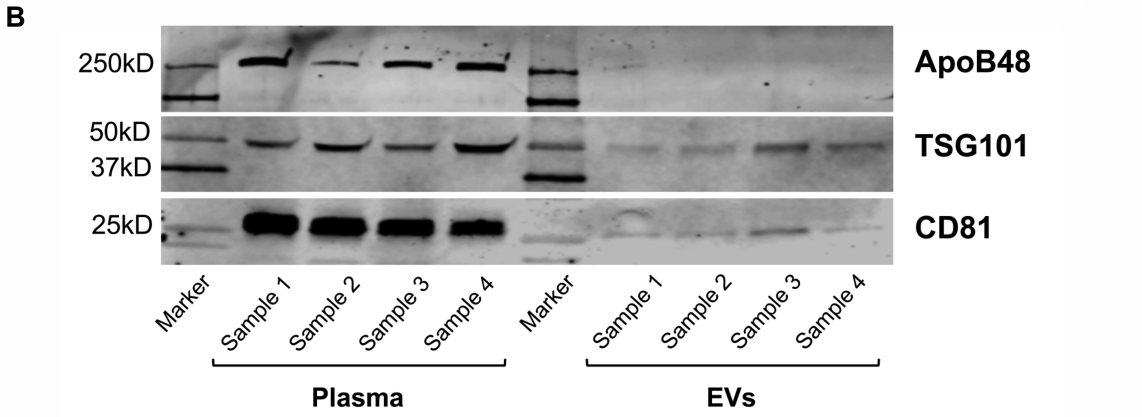
B
250kD
50kD
37kD
25kD
ApoB48
TSG101
CD81
Marker
Sample 1
Sample 2
Sample 3
Sample 4
Plasma
EVs

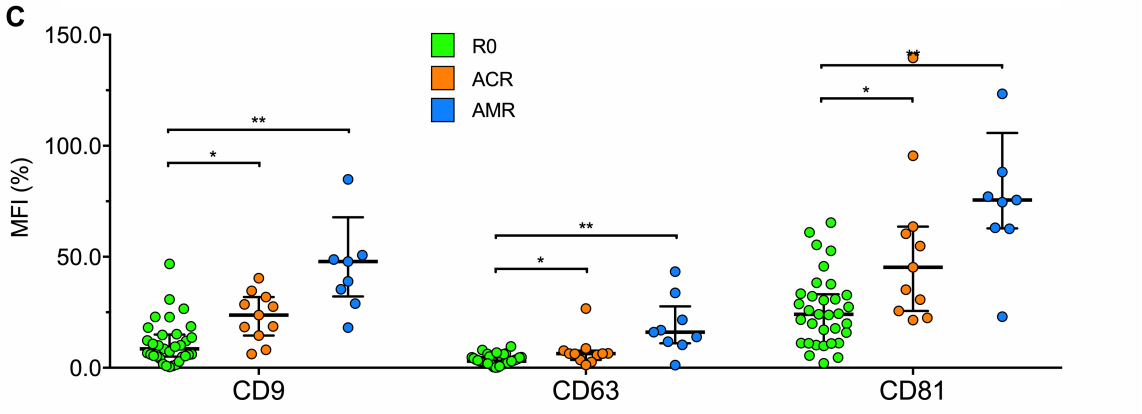
C
R0
ACR
AMR
MFI (%)
CD9
CD63
CD81

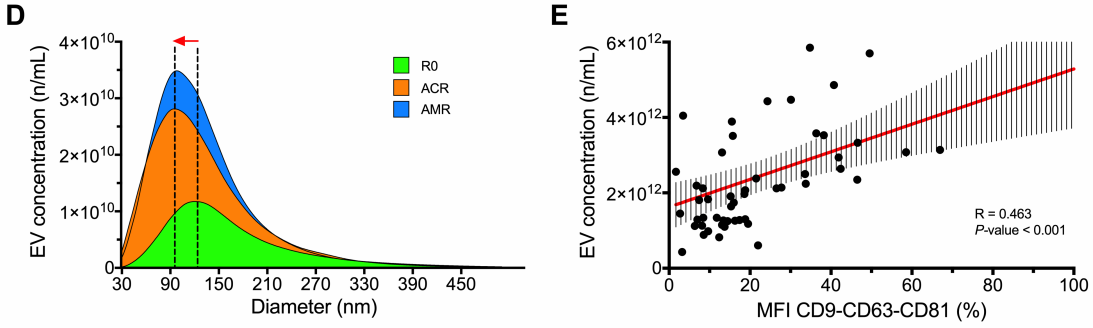
D
EV concentration (n/mL)
Diameter (nm)
R0
ACR
AMR
E
EV concentration (n/mL)
MFI CD9-CD63-CD81 (%)
R = 0.463
P-value < 0.001

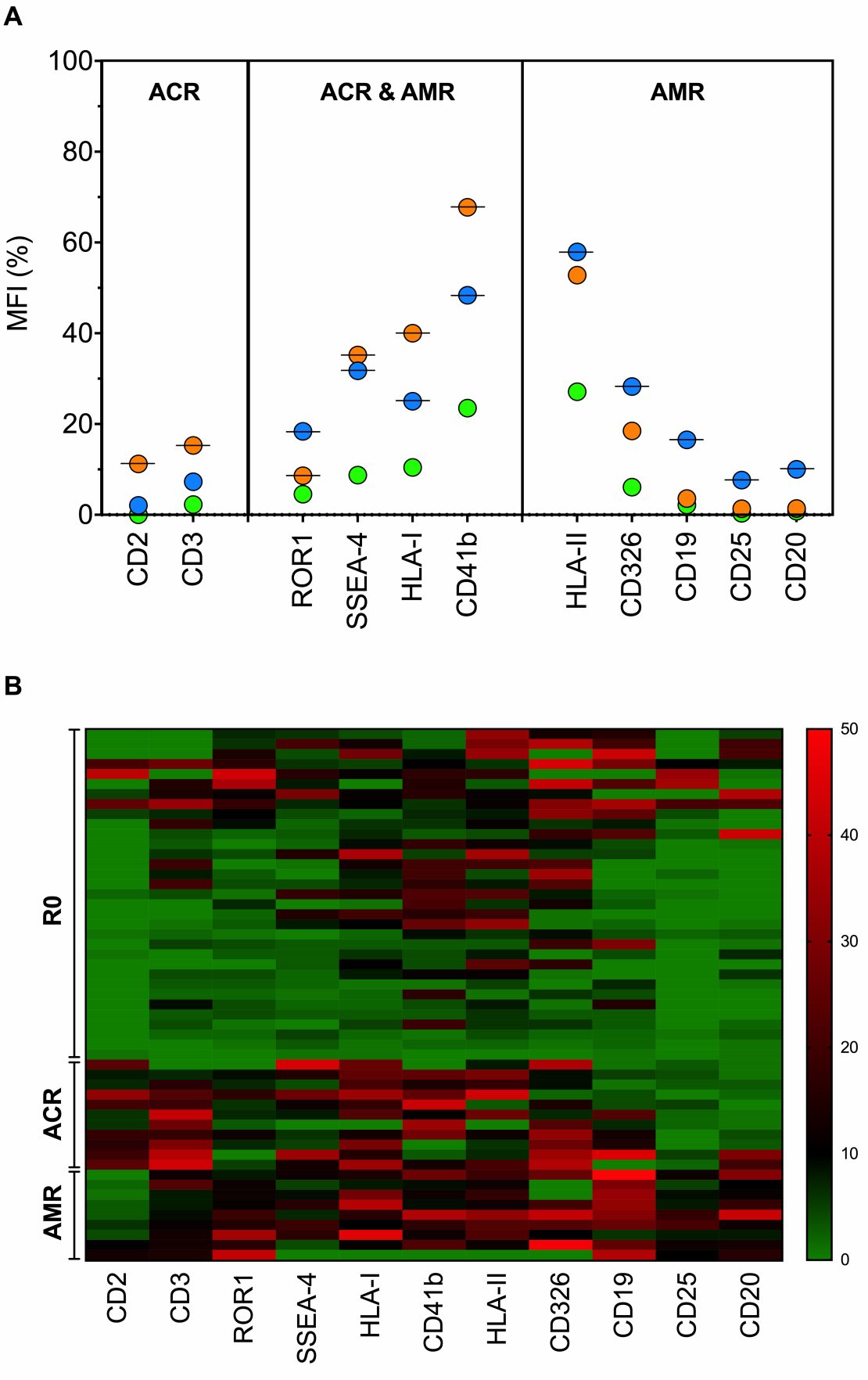
A
100
80
60
40
20
0
MFI (%)
ACR
ACR & AMR
AMR
CD2
CD3
ROR1
SSEA-4
HLA-I
CD41b
HLA-II
CD326
CD19
CD25
CD20
B
R0
ACR
AMR
50
40
30
20
10
0
CD2
CD3
ROR1
SSEA-4
HLA-I
CD41b
HLA-II
CD326
CD19
CD25
CD20

600

A

R0 *vs.* ACR [n=44]	AUC (95% CI)	*P*-value	Sensitivity (%)	Specificity (%)
CD3	0.848 (0.736-0.961)	**0.001**	90.9	75.8
CD2	0.829 (0.704-0.955)	**0.001**	100.0	81.8
ROR1	0.771 (0.627-0.915)	**0.008**	90.9	66.7
SSEA-4	0.832 (0.711-0.952)	**0.001**	100.0	63.6
HLA-I	0.939 (0.869-1.000)	**0.000**	100.0	87.9
CD41b	0.815 (0.653-0.978)	**0.002**	90.9	60.6

B

R0 *vs.* AMR [n=42]	AUC (95% CI)	*P*-value	Sensitivity (%)	Specificity (%)
CD19	0.795 (0.648-0.942)	**0.007**	88.9	78.8
HLA-II	0.788 (0.653-0.922)	**0.009**	100.0	69.7
CD25	0.727 (0.568-0.886)	**0.039**	88.9	75.8
ROR1	0.879 (0.776-0.981)	**0.001**	100.0	75.8
SSEA-4	0.820 (0.692-0.947)	**0.004**	100.0	60.6
HLA-I	0.872 (0.757-0.988)	**0.001**	88.9	75.8
CD41b	0.778 (0.619-0.937)	**0.011**	100.0	51.5
CD326	0.788 (0.597-0.979)	**0.009**	88.9	69.7
CD20	0.798 (0.651-0.945)	**0.007**	88.9	81.8

C

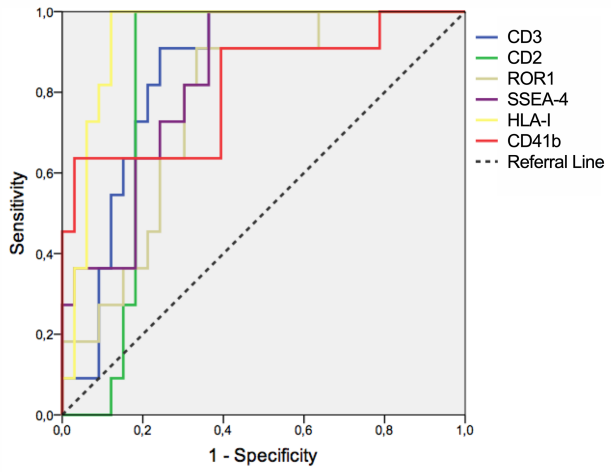

D

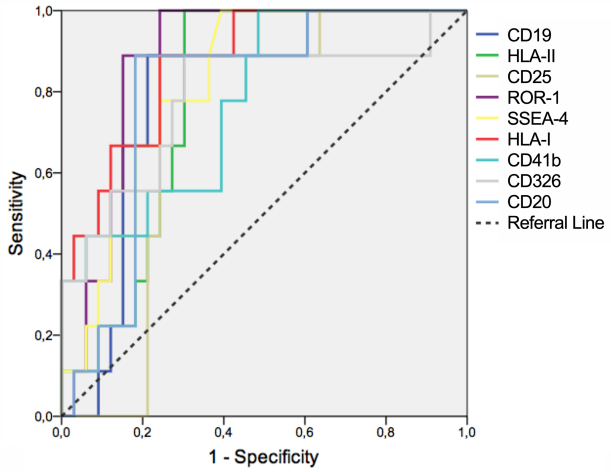

601

A

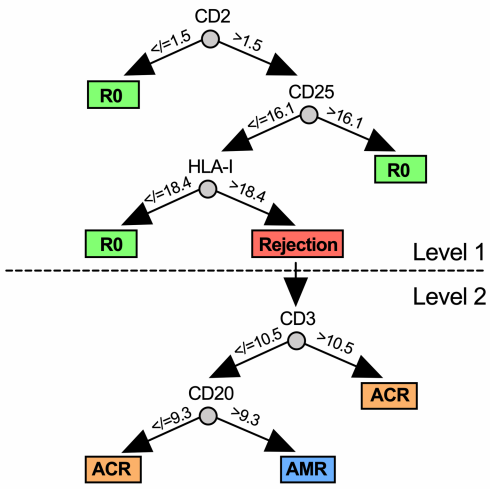

Level 1		DETECTED at TRAINING		INTERNAL VALIDATION	
		R0	Rejection	R0	Rejection
REAL	R0	**33**	0	**28**	5
	Rejection	0	**20**	1	**19**
Accuracy		100.0%		88.7%	

Level 2		DETECTED at TRAINING		INTERNAL VALIDATION	
		ACR	AMR	ACR	AMR
REAL	ACR	**11**	0	**10**	1
	AMR	1	**8**	2	**7**
Accuracy		95.0%		85.0%	

B

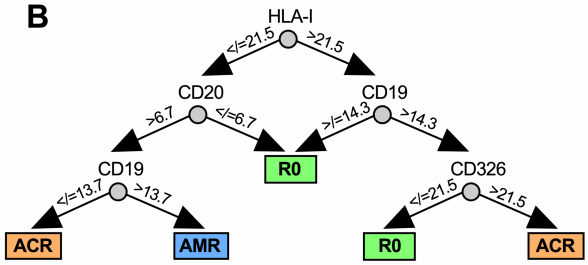

Combined		DETECTED at TRAINING			INTERNAL VALIDATION		
		R0	ACR	AMR	R0	ACR	AMR
REAL	R0	**33**	0	0	**27**	0	6
	ACR	0	**11**	0	0	**10**	1
	AMR	0	0	**9**	1	1	**7**
Accuracy		100.0%			83.0%		

602

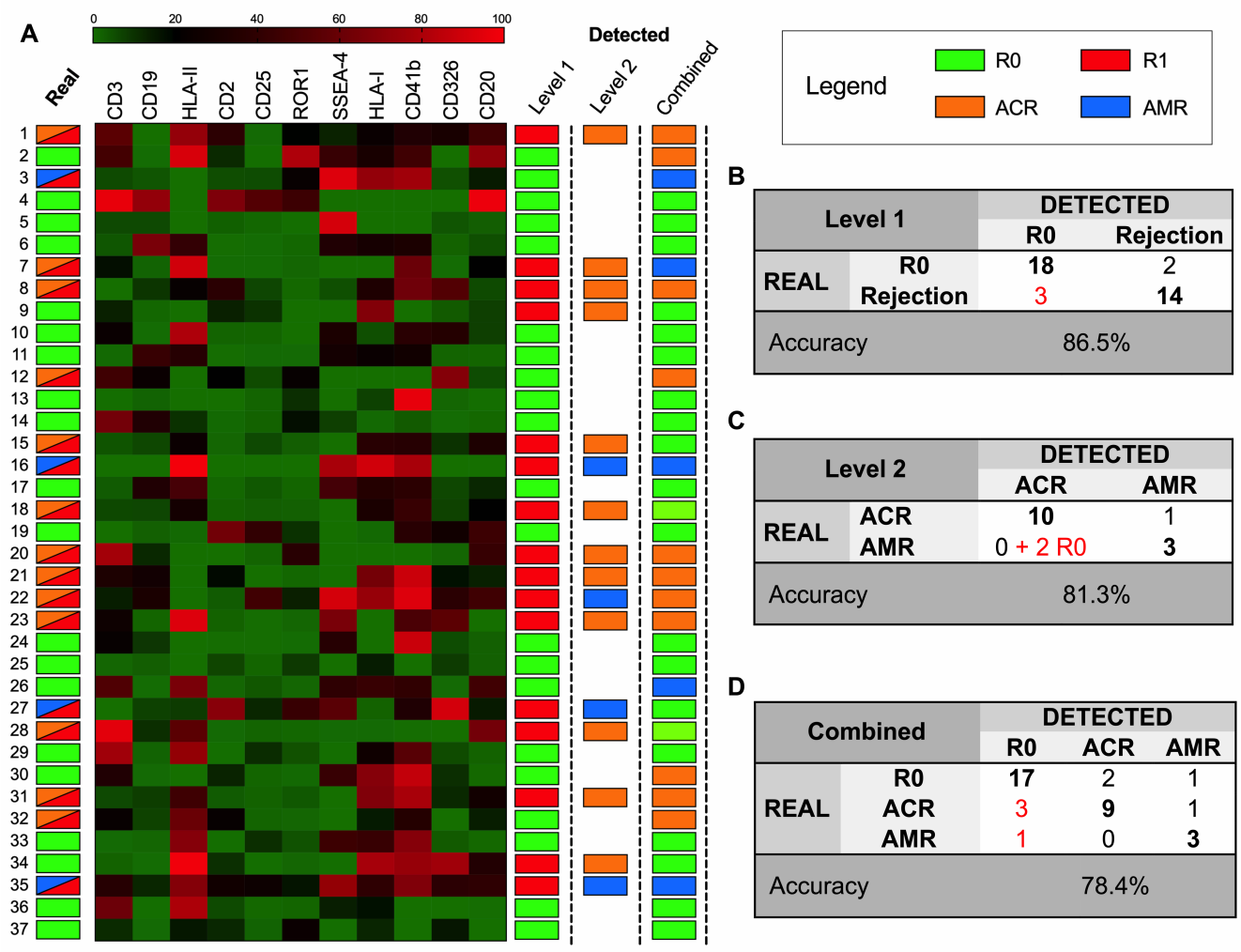

B

Level 1		DETECTED	
		R0	Rejection
REAL	R0	18	2
	Rejection	3	14
Accuracy		86.5%	

C

Level 2		DETECTED	
		ACR	AMR
REAL	ACR	10	1
	AMR	0 + 2 R0	3
Accuracy		81.3%	

D

Combined		DETECTED		
		R0	ACR	AMR
REAL	R0	17	2	1
	ACR	3	9	1
	AMR	1	0	3
Accuracy		78.4%		

603

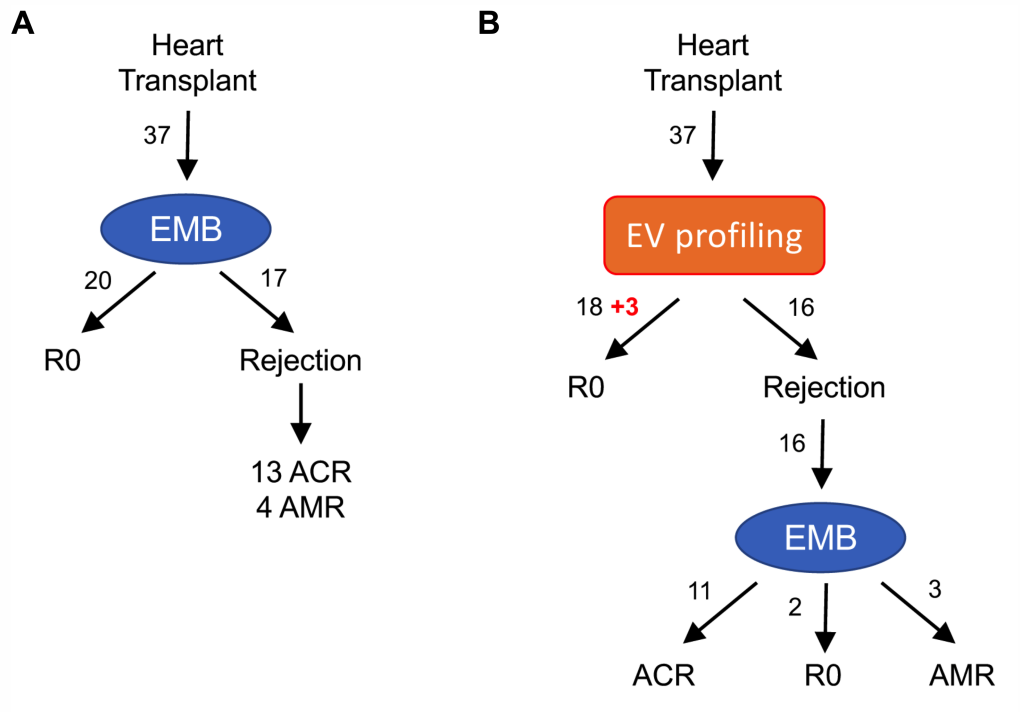
A
Heart
Transplant
37
EMB
20
17
R0
Rejection
13 ACR
4 AMR
B
Heart
Transplant
37
EV profiling
18 +3
16
R0
Rejection
16
EMB
11
2
3
ACR
R0
AMR